Exp Oncol 2019
41, 1, 46–52

Experimental ONCOLOGY

EVALUATION OF DOSE CALCULATION ALGORITHMS USING DIFFERENT DENSITY MATERIALS FOR IN-FIELD AND OUT-OF-FIELD CONDITIONS

*S. Alghamdi, A. Tajaldeen**
Radiological Sciences Department, College of Applied Medical Science,
Imam Abdulrahman Bin Faisal University, Dammam 31441, Saudi Arabia

***Aim*: The accuracy of the dose calculation is vital in the stereotactic ablative body radiotherapy (SABR) technique to achieve clinically effective dose distribution for better tumor control. Multiple commercial radiotherapy treatment planning systems (TPS) were implemented with different algorithms, such as Acuros XB in Eclipse and Superposition in XiO. The aim of this study is to investigate five different dose calculation algorithms, namely, pencil beam convolution (PBC), Acuros XB, AAA implemented in an Eclipse system, collapsed cone convolution (CCC) algorithm implemented in Mobius3D and superposition algorithms implemented in the XiO system, and then validate the results against measurements using an Institute of Physical Sciences in Medicine (IPSM) phantom with different density materials for in-field and out-of- field conditions. *Material and Methods:* The IPSM phantom was used to investigate the dose calculation algorithm performances in four different densities (water, lung, ribs, and dense bone) using different beam configurations, including small beam fields utilised in lung SABR. Five commercial algorithms implemented in two TPS (Eclipse and XiO) and one plan check (M3D) system were used for in-field and out-of-field measurement. *Results*: In the in-field condition, the Acuros XB algorithm had lower mean differences than the measured dose by the IC ranging from −0.46 to 0.24 for all the densities. In the out-of-field condition, the results of eclipse system: AAA, PBC and Acuros XB algorithms demonstrated underdose point's measurements by −40% for all densities except for AAA calculations in lung density (overdosed by 40%). The measured points of the superposition algorithms were overestimated to the actual dose less than 30% in water, lung and dense bone. At the same densities, the CCC algorithms showed relatively the lowest differences in percentage compared to the superposition algorithms. *Conclusion*: Our results showed that the Acuros XB and superposition algorithms are closer to the actual measured dose than AAA, PBC and CCC for majority of the field conditions for water-equivalent, lung, rib and dense bone densities. The CCC algorithm resulted in a better agreement with the measurement of the out-of-field points compared with the other algorithms.**

***Key Words*: 3D conformal radiotherapy, stereotactic ablative body radiotherapy, collapsed cone convolution algorithm, in-field condition, out-of-field condition.**

Dose calculation algorithms play an important role in delivering the precise dose to the target volume. Prior to clinical use, the accuracy of dose calculation algorithm needs to be validated against measurements for different inhomogeneous conditions. The ideal dose calculation algorithms should perfectly reflect the actual dose distribution in the patient to help assess treatment plans with low uncertainty. According to the International Commission on Radiation Units and Measurements (ICRU) recommendations, the delivered dose should have an error of less than 5% [1], which suggests that every step of dose calculation and patient positioning, among others, should be performed far better than this percentage. Moreover, the required accuracy for the dose calculation step should be in the range of 2–3% [2].

At present, Monte Carlo (MC) simulations are considered the most accurate algorithms by simulating large numbers of primary photon histories [3]. However, the main disadvantage of such algorithms is their relatively long processing time, which makes them less attractive in daily clinical applications [4]. Consequently, many treatment planning system (TPS) vendors have attempted to develop clinical algorithms that can calculate the dose distribution with a reasonable processing time. Semi-analytical algorithms for the dose calculation of photon beams, including pencil beam convolution (PBC) [5], anisotropic analytical algorithms (AAA) [5] and superposition/convolution algorithms such as superposition [4] and collapsed cone convolution (CCC) [6], are widely used in radiation therapy centres. These algorithms can provide relatively accurate measurements of the dose distribution of the target volume with less processing time [7]. Several previous studies investigated the performances and limitations of these algorithms in phantoms composed of water or water — air interfaces (large inhomogeneities) to mimic lung cases [7–11]. According to the existing literature, no study has yet examined the performances of different algorithms using four different densities in a phantom using a number of beam geometries with different field sizes, including symmetric and asymmetric fields.

This study investigated five different dose calculation algorithms, namely, PBC, Acuros XB, AAA implemented in an Eclipse system, CCC algorithm implemented in Mobius3D and superposition algorithms implemented in the XiO system, and then validated the results against measurements using an Institute of Physical Sciences

Submitted: September 25, 2018.
*Correspondence: E-mail: atajaldeen@gmail.com
Abbreviations used: AAA – anisotropic analytical algorithms; CCC – collapsed cone convolution; CT – computed tomography; IC – ion chamber; IPSM – Institute of Physical Sciences in Medicine; MC – Monte Carlo; PBC – pencil beam convolution; SABR – stereotactic ablative body radiotherapy; TPS – treatment planning systems.

in Medicine (IPSM) phantom with different density materials for in-field and out-of- field conditions.

MATERIALS AND METHODS

A phantom designed by the IPSM Radiotherapy Topic Group [12] was used to study the accuracy of dose calculation algorithms. It is made of epoxy-resin (water-equivalent material) and it consists of six removable water-equivalent rods that are 3 cm in diameter and that can be substituted by ion chamber (IC) [12]. In this study, the rods were substituted with the IC for all measurements (Fig. 1). The phantom also has a 9-cm water-equivalent insert that can be replaced by other material inserts that are equivalent to the lung, rib and dense bone (Fig. 1, *a–d*). In this study, the dose measurements were conducted using a 0.6 cc IC.

Each density insert simulates real clinical densities with a similar CT number. The CT number was assigned as follows: water insert (CT number = 0), lung insert (CT number = −740 to −770), rib insert (CT number = 400) and dense bone insert (CT number = 1000). The

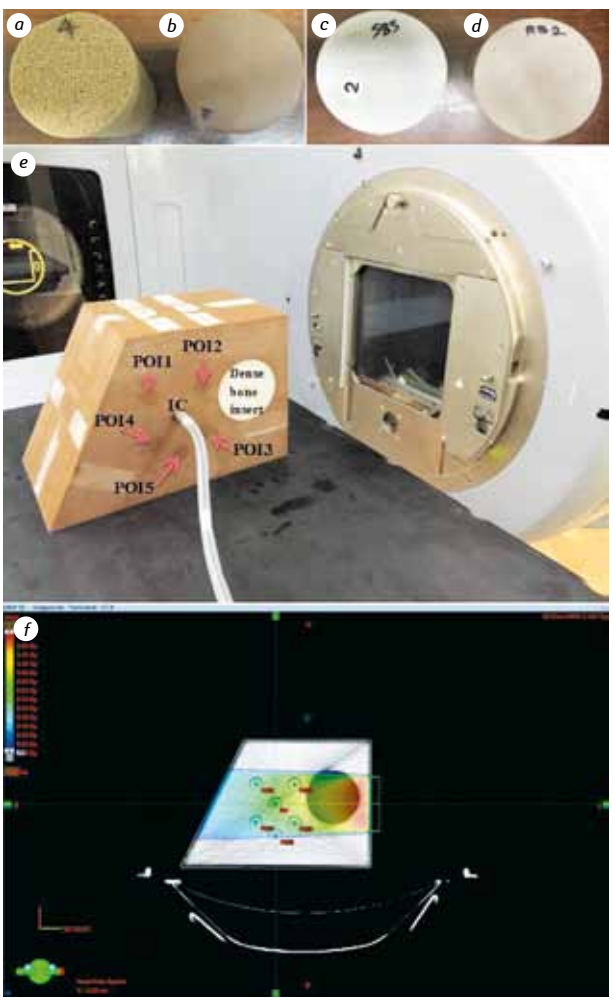

Fig. 1. Images of different density inserts for the IPSM phantom: (*a*) lung density insert; (*b*) water density insert; (*c*) dense bone insert; and (*d*) rib density insert. The IPSM phantom is illustrated in *e* and *f*. (*e*) The IPSM phantom with the dense bone insert and the gantry angle of 90°. The IC is placed at the ISO point. (*f*) A computed tomography (CT) image of the IPSM phantom with the lung density insert displayed in Eclipse-TPS; it has six points: ISO, POI1, POI2, POI3, POI4 and POI5. The CT image demonstrates the beam field of 10 × 10 with gantry angle 90°

IC was placed at six different positions, and three different field sizes of 3 × 5, 5 × 5 and 10 × 10 were defined to provide both in-field and out-of-field measurements. The in-field measurements were represented by the calculated point (ISO), and the out-of-field measurements were allocated for (POI5) for beams 1–12. These measurements were performed for different beam configurations as follows: open, physical wedge (Phy) and enhanced dynamic wedge (EDW) fields at 90° and 270° gantry angles with a collimator angle of 90°. The applied monitor unit (MU) for all points and beams geometries was 100 MU. All calculations were performed for Varian 21iX linear accelerator 6 MV photons (Varian Medical System, Palo Alto, CA). The beam configurations of the gantry, collimation and MU were consistent in all calculations.

The clinical treatment plans were initially created using the Eclipse TPS (v13.6, Varian Medical Systems) with the same beam configurations utilised in the IC measurements. In the Eclipse system, the doses were recalculated by AAA (v13.6.23), PBC (v11.0.31) and Acuros XB (v13.6.23) algorithms. The AAA algorithm utilises pencil-beam energy deposition kernels produced from the MC simulation [5, 6]. These algorithms represent the kernels analytically and adopt a scaling based on local density variations using specific analytic kernels for build-up or down effects at density interfaces [5, 6]. In the PBC algorithms, the dose kernels at a point are summed up along a line in a phantom to acquire a pencil-type beam (or dose distribution) [13]. Using a convolution method, the pencil beam computes the dose distribution around an infinitely small beam in water. Unlike the AAA, the PBC algorithms cannot consider the variation of lateral scattering effects [13]. The Acuros XB algorithm has been implemented recently in the Eclipse system [14]. They are based on the explicit solution of linear Boltzman transport equations (LBTEs) to demonstrate the dose calculations [14]. The main difference between the MC simulation and the Acuros XB is that the former method solves the coupled system of LBTEs stochastically using the histories of the photon and electron transportation, whereas the latter uses grid-based LBTE solutions to separate the photon and electron influences in energy, space and angle and determines a solution for the radiation transport through matter [15]. The Acuros XB algorithms have a relatively less processing period when calculating the dose than the MC simulation, and their results are comparable with those of the MC [16].

The DICOM RT plans and CT images of the IPSM phantom were imported into the XiO TPS (v5.0, Elekta AB, Stockholm, Sweden) and Mobius Medical System (M3D; v2.0.1, Mobius Medical system) to recalculate the measured points using superposition and CCC algorithms respectively. The M3D uses the CCC algorithm, which adopts the convolution of a total energy released per unit mass (TERMA) volume with MC-derived point spread kernels implemented in a graphic processing unit [6, 17]. The superposition algorithm implemented

in the XiO-TPS involves the convolution of the TERMA volume with MC-measured point energy deposition kernels [6]. It is characterised by density scaling of the energy deposition kernels to consider the local density heterogeneity [6].

The measured dose by the IC (the actual dose) was compared with the dose calculation derived from the TPS for the AAA, PBC, Acuros XB, superposition and CCC algorithms. To evaluate the performance of the algorithms, the actual dose by the IC was used as the reference dose. The differences in percentages for all calculated points by the five algorithms were normalised to the reference dose. All calculated points were defined as follows: [(the measured dose calculated by the algorithms — the measured dose by the IC/the measured dose by the IC)].

The statistical analyses were performed by Graph Pad PRISM 6 software, v. 6.03. A one-way ANOVA, with repeated measures utilising multiple comparisons was used to investigate the statistical significances ($p < 0.05$) and mean differences among the five algorithms in four different densities (water, lung, ribs, and dense bone).

RESULTS

The measurement points for the measured dose by IC and the five algorithms for water, lung and dense bone density — IPSM inserts are shown in Table 1. The measurement points for rib density insert are shown in Table 2. Theses tables include the beam configurations, field size, gantry angle and wedge application. The results can be divided into in-field and out-of-field results as follows.

Table 1. Measurement points for the measured dose by IC and the five algorithms (AAA, PBC, Acuros XB, Superposition and CCC) using water, lung, and dense bone density inserts in IPSM phantom for different beam configurations

Beams	Gantry	Field size	Wedge	Measurement points
Beam 1	90°	10 × 10 cm²	None	ISO
		SSD = 100 cm		POI1
				POI2
				POI3
				POI4
Beam 2	90°	10 × 10 cm²	EDW 25° OUT	ISO
				POI1
				POI2
				POI3
				POI4
Beam 3	90°	5 × 5 cm²	None	ISO
Beam 4	90°	5 × 5 cm²	EDW 25° OUT	ISO
Beam 5	90°	5 × 5 cm²	45° OUT (Phy)	ISO
Beam 6	270°	5 × 5 cm²	None	ISO
Beam 7	270°	5 × 5 cm²	EDW 25° IN	ISO
Beam 8	270°	5 × 5 cm²	45° IN (Phy)	ISO
Beam 9	90°	3Y × 5X cm²	None	ISO
Beam 10	90°	3Y × 5X cm²	45° OUT (Phy)	ISO
Beam 11	270°	3Y × 5X cm²	None	ISO
Beam 12	270°	3Y × 5X cm²	45° IN (Phy)	ISO

Note: The collimator is set to 90° for all beams. Phy – physical wedge; EDW – enhanced dynamic wedge.

In-field condition

The water density results showed a maximum percentage of ± 1% for all algorithms (Fig. 2, *a*). The Acuros XB and superposition algorithms represented the lowest mean values of 0.2 and 0.31, respectively (Table 3). In the rib density material, the calculation differences in the algorithms ranged from −1.27%

Table 2. Measurement points for the measured dose by IC and the five algorithms (AAA, PBC, Acuros XB, Superposition and CCC) using a rib insert – IPSM phantom for different beam configurations

Beams	Gantry	Field size	Wedge	Measurement points
Beam 1	90°	10 × 10 cm²	None	ISO
		SSD = 100 cm		POI1
				POI2
				POI3
				POI4
Beam 2	90°	10 × 10 cm²	EDW 25° OUT	ISO
				POI1
				POI2
				POI3
				POI4
Beam 3	90°	5 × 5 cm²	None	ISO
Beam 4	90°	5 × 5 cm²	EDW 25° OUT	ISO
Beam 5	90°	5 × 5 cm²	45° OUT (Phy)	ISO
Beam 9	90°	3Y × 5X cm²	None	ISO
Beam 10	90°	3Y × 5X cm²	45° OUT (Phy)	ISO

Note: The collimator set to 90° for all beams. Phy – physical wedge; EDW – enhanced dynamic wedge.

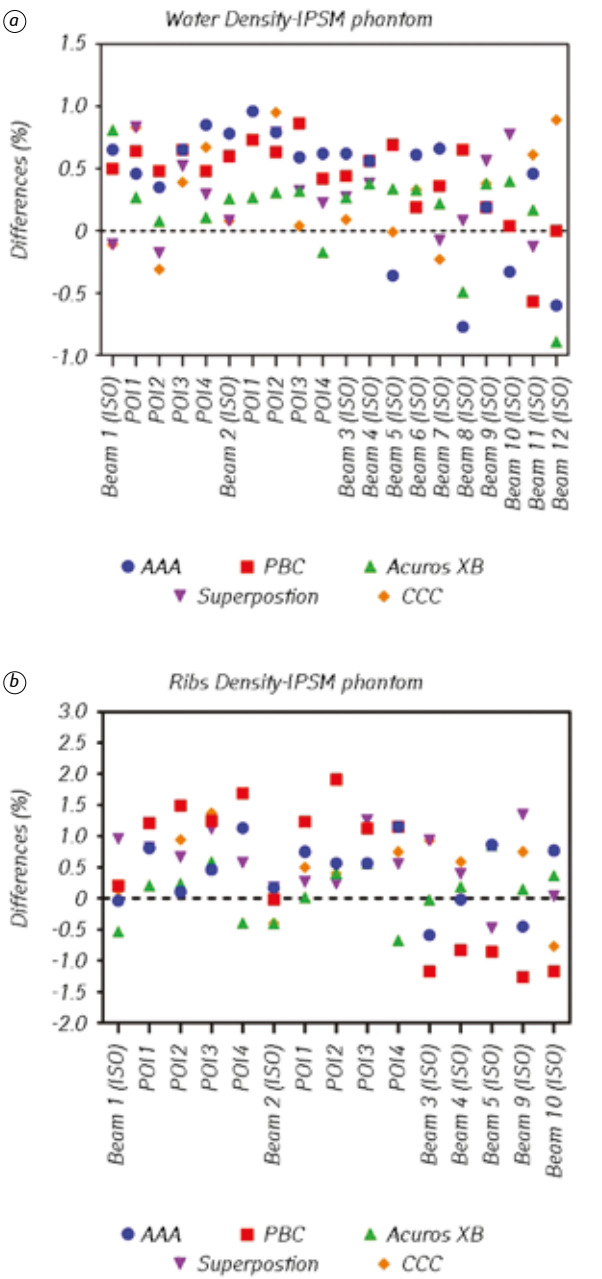

Fig. 2. Percentages differences of the calculated points for five algorithms compared with the measured dose from the IC for (*a*) water and (*b*) rib density inserts

Table 3. Mean differences in percentage of different densities: water, lung, rib and dense bone for gantry angles of 90° and 270°

	AAA	PBC	Acuros XB	Superposition	CCC	*p* value
Water density	0.39 ± 0.49	0.43 ± 0.32	0.2 ± 0.36	0.31 ± 0.33	0.36 ± 0.39	0.0010
Lung density	1.12 ± 1.23	0.38 ± 1.06	0.22 ± 0.91	0.36 ± 0.87	0.49 ± 0.69	0.0003
Rib density	0.42 ± 0.52	0.39 ± 1.14	0.11 ± 0.43	0.58 ± 0.48	0.52 ± 0.68	0.0163
Dense bone density (90° beams)	0.41 ± 0.93	1.57 ± 1.15	0.24 ± 0.88	3.2 ± 1.44	3.01 ± 1.51	< 0.0001
Dense bone density (270° beams)	–0.44 ± 0.32	–1.68 ± 0.77	–0.21 ± 0.23	0.08 ± 0.36	1.34 ± 0.33	0.0243

Note: The data presented in this table was the result of three independent measurements (n = 3). The mean values (mean values ± standard deviation) are significantly different among the five algorithms ($p < 0.05$, one-way analyses of variance (ANOVA) with repeated measures).

to 1.91% (Fig. 2, *b*), and the mean differences did not exceed 0.58% (Table 3).

The performance of the algorithms in dense bone density showed significant differences between the 90° and 270° gantry angles. In 90° gantry angle, the PBC, superposition and CCC algorithms experienced maximum error percentages in the following points of beam 1: POI2 = 3.55% in PBC, POI1 = 4.88% in Superposition and POI1 = 5.3% in CCC, respectively (Fig. 3, *a*). These maximum error percentages were associated with high mean differences of 1.57 ± 1.15, 3.2±1.44 and 3.01 ± 1.51 for the PBC, superposition and CCC algorithms, respectively (Table 3). By contrast, the AAA and Acuros XB algorithms provided better performance in dense bone density with maximum error differences only in particular points of beam 1 as follows: POI1 = 2.32% and POI2 = 1.45%, respectively (Fig. 3, *a*). At 270° gantry angle, the five measured points of all algorithms except for the PBC algorithm showed maximum differences of (< ± 1.83%) that ranged between –0.9% and 1.83% (Fig. 3, *b*). The performance of the PBC algorithm at a 270° angle was an underestimated dose compared with the measured dose by the farmer chamber with a maximum percentage of –2.87% (Fig. 3, *b*).

In the lung density measurements, the differences in percentages of the five algorithms were within ± 2%. However, some points of the AAA and PBC measured points downstream from the measured dose were beyond 2%. Four points of the AAA assigned to POI1 and POI2 of beams 1 and 2 experienced high errors at 2.13%, 3%, 2.82% and 3.65%, respectively. The PBC had two points 2.13% and 2.99% related to POI1 for beams 1 and 2, respectively that exceeded 2% (Fig. 4). As shown in Fig. 3, *a*, the calculations of Acuros XB were close to the measured dose by the IC and associated with the lowest mean values 0.22 and –0.46 for lung densities (Table 3). Table 3 summarises the mean values of the five algorithms with four different densities inserts: water, lung, ribs and dense bone. The statistical

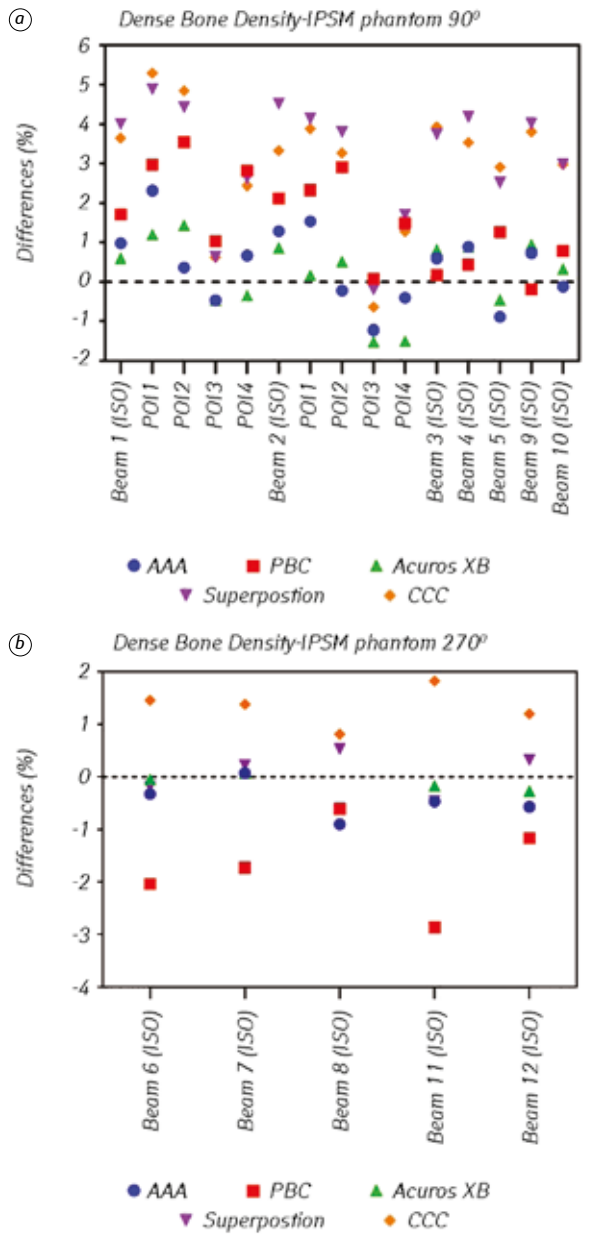

Fig. 3. Percentages differences of the calculated points for five algorithms compared to the measured dose from the IC for dense bone density at (*a*) 90° and (*b*) 270°

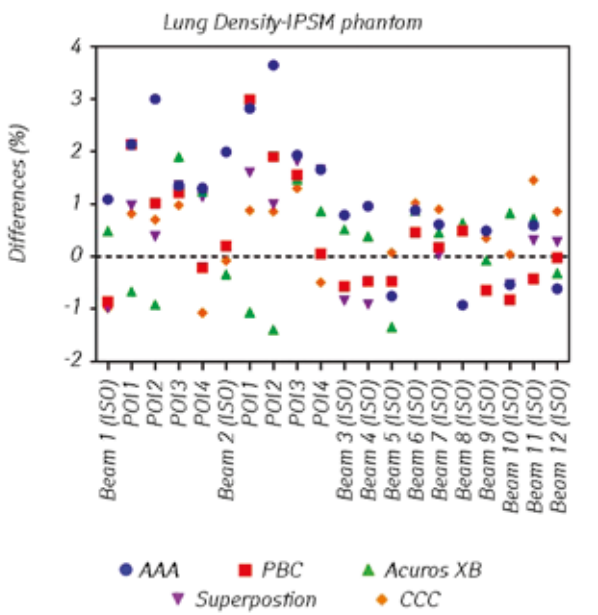

Fig. 4. Percentages differences of the calculated points for five algorithms compared to the measured dose from the IC for lung density

analysis was significant for the mean differences among the four densities with $p < 0.05$.

Out-of-field condition

The differences in percentages for the five algorithms measurements in out-of-field condition for four different densities were shown in Fig. 5, *a*–*d*. The results of eclipse system: AAA, PBC and Acuros XB algorithms demonstrated underdose point's measurements by –40% for all densities except for AAA calculations in lung density (overdose by 40%). The measured points of the superposition algorithms were overestimated to the actual dose less than 30% in water, lung and dense bone (Fig. 5, *a*, *b* and *d*). At the same densities, the CCC algorithms showed relatively the lowest differences in percentage compared to the superposition algorithms. Compared to the actual dose, most of the measured points by CCC were less than 25% in water and lung density while the dense bone results showed most of the measured doses were close to the actual dose results except for four points were beyond –20% (Fig. 5, *a*, *b* and *d*). In the rib density, the calculated points of the superposition and CCC algorithms were underestimated to the actual dose by less than –30% except for two points in superposition calculation were overestimated by 25% and 30%, respectively. Similarly to the dense bone results of the CCC, most of the measured points of the CCC calculation in the rib density were close to the actual dose (Fig. 5, *c*, *d*). The highest discrepancies (–71%) were allocated for beam 12 representing small field (Y = 3, X = 5) using physical wedges (45° IN) in the dense bone density for all calculated algorithms except superposition algorithms (Fig. 5, *d*).

DISCUSSION

This study investigated the performances of five algorithms, namely, AAA, PBC and Acuros XB in Eclipse,

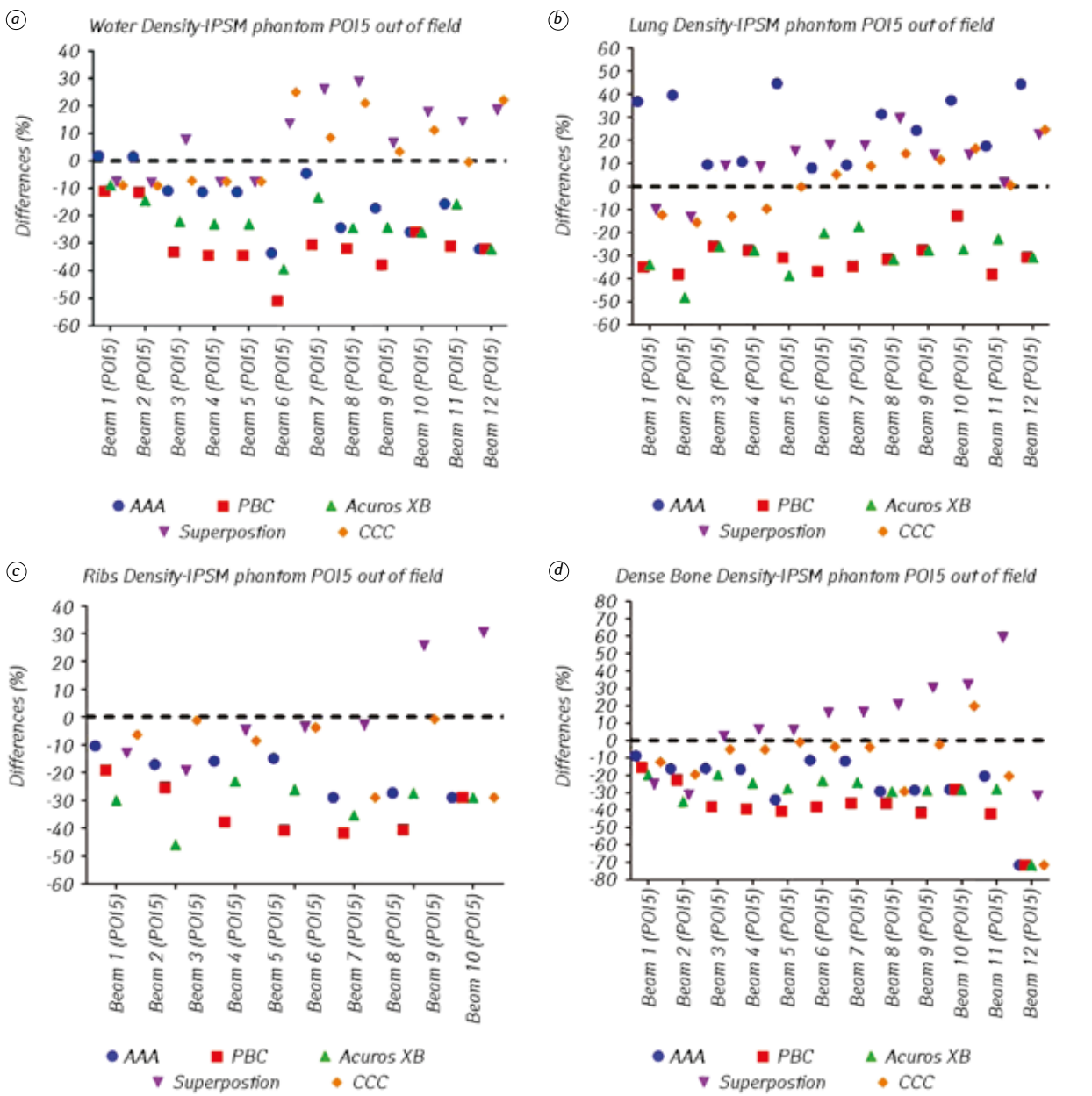

Fig. 5. Percentages differences of the calculated points for five algorithms in out-of-field condition of four different densities: (*a*) water density, (*b*) lung density, (*c*) rib density and (*d*) dense bone density

Superposition in XiO TPS and CCC implemented in plan-checking software (Mobius3D). The comparison between the absolute doses from the IC (the measured dose) and the calculated doses by the five algorithms showed a significant variation for the different densities of water, lung, rib and dense bone. The discussion section can be divided as follows:

In-field condition

In water density, the measurements of the five algorithms demonstrated almost similar performances as predicted in a homogenous medium. PBC and AAA are considered semi-analytical algorithms [18] that can provide a lower uncertainty (within ± 1%) in homogenous tissues than in heterogeneous tissues [4]. The calculations of the five algorithms for rib density were within ± 2%. Both water and rib densities showed relatively small mean differences for all calculations including in-field measurements. By contrast, the dose calculation performances demonstrated a significant variation in calculating dose for the lung and dense bone densities. In the lung density, the AAA and PBC algorithms recorded the largest differences compared with the measured dose and exceeded 2% for beams 1 and 2, respectively. Acuros XB, superposition and CCC provided better performances than AAA and PBC in the calculation of lung densities with differences less than 2%.

The dense bone density for the beams with a 90° gantry angle showed the largest discrepancies for PBC, superposition and CCC. As the measured doses were located after the dense bone, these discrepancies of the algorithms could be explained as a limitation in the accuracy of the mass attenuation data utilised in the TERMA calculations for these algorithms. The calculation of all algorithms provided better performances for beams with a 270° gantry angle because of the absence of the high attenuation of the dense bone. However, the PBC calculations of small fields, namely, beam 6 (5 × 5) and beam 11 (3 × 5), for the same gantry angle under-predicted the absolute dose and exceeded −2%. AAA, Acuros XB and PBC showed almost the same mean difference in percentage in the 90° and 270° gantry angles. For example, the mean difference of the PBC results with a 90° (1.57%) was almost the same as the mean difference of those with a 270° (−1.68%), but the downstream points were in the opposite direction. This result demonstrated that PBC provided high discrepancies within (± 1.7%) in both gantry angles compared with AAA and Acuros XB.

Hardcastle *et al*., 2016 [6] compared the AAA and CCC algorithms for 10 lung cancer patients, used the in-house MC algorithm as a reference calculation, and showed that CCC closely agreed with the MC algorithms [6]. For the 10 patients, the calculated doses were at the centre of the ITV [6]. The maximum differences in AAA and CCC compared with MC were −11.3% and 7.5%, respectively [6]. The results from our study were consistent with those of Hardcastle *et al*., 2016 [6]. CCC provided lower mean differences in absolute dose by (0.49%) compared with AAA (1.12%) in the lung density. Moreover, *Tan et al*., 2014 [7] investigated the accuracy of six algorithms (i.e., AAA, PBC, Acuros XB, FFT convolution, superposition and MC algorithms) in calculating the entrance and exit doses for 6 MV in a water phantom [7]. They found that the entrance dose measurements agreed within 2% of the measured dose by the IC [7]. These results were consistent with those of our investigation using water density, as the measurements of 20 points were close to the IC measurements and the differences were within ± 1%. However, the performances of the six algorithms varied when computing the exit doses in the same phantom. The exit doses computed by the FFT convolution, superposition, Acuros XB and MC algorithms were close to the measured dose, and their percentages ranged from 2% to 3% [7]. By contrast, the exit doses computed by AAA and PBC were higher than the measured dose (IC) by up to 4.8% and 5.3%, respectively [7]. The reason for this outcome is that AAA and PBC assumed that the full backscatter existed even at the exit level, thus resulting in the over-prediction of exit doses [7]. Our results agreed with the good performance results of Acuros XB and superposition in Tan *et al*., 2014 [7]. Despite the high mean difference in the superposition algorithm when calculating the dense bone with 90° beams, superposition and Acuros XB provided the lowest mean difference and thus produced close values to the actual dose by IC for all densities. Another study compared superposition and AAA for four different cancer sites, namely, brain, nasopharynx, lung and prostate, and found that the mean dose deviation of superposition was within 3% and was relatively more accurate than that of AAA, especially in a heterogeneous medium [4]. Moreover, this study agreed with our results in that AAA had relatively high mean differences (1.12%) compared with the other algorithms in a lung density-IPSM phantom. According to Stathakis *et al*., 2012 [16] the dose prediction accuracy of Acuros XB in bone and lung heterogeneities is better than those of AAA and CCC and is in good agreement with the MC measurements [16].

Out-of-field condition

In the out-of-field condition, superposition and CCC provided lower discrepancies than AAA, PBC and Acuros XB. The calculated doses of AAA, PBC and Acuros XB were underestimated by less than −40% for most of the calculated points compared with the actual dose in the out-of-field condition for all densities. Our results agreed with those of Howell *et al*., 2010 [19]. They quantified the accuracy of the out-of-field condition using the AAA algorithms and the results showed an underestimation (about 40%) of the measured dose compared with the actual dose [19]. The same research group suggested that the underestimation of the dose increased with the increasing distance from the field edge [19]. The results from our study showed that the beam configurations affected the measured doses for all densities. Beams with a larger field size without using enhanced or physical wedges

provide fewer discrepancies in percentages than beams with a small field size using wedges. Moreover, these percentages increased with the physical wedges associated with an asymmetric small field size (Y = 3, X = 5) in dense bone density (Fig. 5, *d*). The out-of-field results for the previous algorithm calculations can be used in low doses outside the irradiation target, which can cause acute toxicities [19]. The low-dose information can be used for the assessment of late effects, such as second cancers. According to *Kry et al.*, 2007 [20] a 50% change in low dose is sufficient to cause a significant variation in second cancer risk [20].

CONCLUSION

Our results showed that the Acuros XB and superposition algorithms are closer to the actual measured dose than AAA, PBC and CCC for majority of the field conditions for water-equivalent, lung, rib and dense bone densities. The CCC algorithm resulted in a better agreement with the measurement of the out-of-field points compared with the other algorithms.

REFERENCES

1. ICRU. Determination of absorbed dose in a patient irradiated by beams of X or gamma rays in radiotherapy procedures. Int Commission on Radiation Units and Measurements, Bethesda, MD, 1976: Report No 24.

2. Fraass B, Smathers J, Deye J. Summary and recommendations of a National Cancer Institute workshop on issues limiting the clinical use of Monte Carlo dose calculation algorithms for megavoltage external beam radiation therapy. Med Phys 2003; **30**: 3206–16.

3. Li JS, Pawlicki T, Deng J, *et al.* Validation of a Monte Carlo dose calculation tool for radiotherapy treatment planning. Phys Med Biol 2000; **45**: 2969.

4. Vincent W, Teddy K, Cola L, *et al.* A comparison between anisotropic analytical and multigrid superposition dose calculation algorithms in radiotherapy treatment planning. Med Dosimetry 2013; **38**: 209–14.

5. Van Esch A, Tillikainen L, Pyykkonen J, *et al.* Testing of the analytical anisotropic algorithm for photon dose calculation. Med Phys 2006; **33**: 4130–48.

6. Hardcastle N, Oborn B, Haworth A. On the use of a convolution-superposition algorithm for plan checking in lung stereotactic body radiation therapy. J Appl Clin Med Physics 2016; **17**: 99–110.

7. Tan YI, Metwaly M, Glegg M, *et al.* Evaluation of six TPS algorithms in computing entrance and exit doses. J Appl Clin Med Phys 2014; **15**: 229–40.

8. Oyewale S. Dose prediction accuracy of collapsed cone convolution superposition algorithm in a multi-layer inhomogenous phantom. Int J Cancer Ther Oncol 2013; **1**: 01016.

9. Carrasco P, Jornet N, Duch M, *et al.* Comparison of dose calculation algorithms in phantoms with lung equivalent heterogeneities under conditions of lateral electronic disequilibrium. Med Phys 2004; **31**: 2899–911.

10. Davidson S, Ibbott G, Prado K, *et al.* Accuracy of two heterogeneity dose calculation algorithms for IMRT in treatment plans designed using an anthropomorphic thorax phantom. Med Phys 2007; **34**: 1850–7.

11. Ojala J, Hyödynmaa S, Barańczyk R, *et al.* Performance of two commercial electron beam algorithms over regions close to the lung-mediastinum interface, against Monte Carlo simulation and point dosimetry in virtual and anthropomorphic phantoms. Phys Med 2014; **30**: 147–54.

12. Thwaites D, Williams JR, Aird EG, *et al.* A dosimetric intercomparison of megavoltage photon beams in UK radiotherapy centres. Phys Med Biol 1992; **37**: 445.

13. Buzdar S, Afzal M, Todd-Pokropek A. Comparison of pencil beam and collapsed cone algorithms, in radiotherapy treatment planning for 6 and 10 MV photon. J Ayub Med Coll Abbottabad 2010; **22**: 152–4.

14. Fogliata A, Nicolini G, Clivio A, *et al.* Dosimetric validation of the Acuros XB Advanced Dose Calculation algorithm: fundamental characterization in water. Phys Med Biol 2011; **56**: 1879.

15. Bush K, Gagne IM, Zavgorodni S, *et al.* Dosimetric validation of Acuros® XB with Monte Carlo methods for photon dose calculations. Med Phys 2011; **38**: 2208–21.

16. Stathakis S, Esquivel C, Quino L, *et al.* Accuracy of the small field dosimetry using the acuros XB dose calculation algorithm within and beyond heterogeneous media for 6 MV photon beams. Int J Med Phys, Clin Engin Radiat Oncol 2012; **1**: 78–87.

17. Childress N, Stephens E, Eklund D, *et al.* Mobius3D white paper: dose calculation algorithm. Mobius Medical Systems (LP Rev. 0), 2012: 1–10.

18. Hasenbalg F, Neuenschwander H, Mini R, *et al.* Collapsed cone and analytical anisotropic algorithm dose calculations compared to VMC++ Monte Carlo simulations in clinical cases. J Phys: Conference Series 2007. IOP Publishing.

19. Howell RM, Scarboro SB, Kry SF, Yaldo DZ. Accuracy of out-of-field dose calculations by a commercial treatment planning system. Phys Med Biol 2010; **55**: 6999.

20. Kry SF, Followill D, White R, *et al.* Uncertainty of calculated risk estimates for secondary malignancies after radiotherapy. Int J Radiat Oncol Biol Phys 2007; **68**: 1265–71.